Ideal-MHD stability of finite-beta plasmas

1979 Nucl. Fusion 19 715

(http://iopscience.iop.org/0029-5515/19/6/003)

IDEAL-MHD STABILITY OF FINITE-BETA PLASMAS

B. COPPI, A. FERREIRA*, J.W.-K. MARK, J.J. RAMOS
Massachusetts Institute of Technology,
Cambridge, Massachusetts,
United States of America

ABSTRACT. An analytical theory of ideal-MHD ballooning modes that can be excited in finite-β equilibria is carried out on model configurations which include the effects of the increase of the poloidal field toward the outer edge of the plasma column and the dependence of the rate of magnetic shear on the poloidal angle. The relevant growth rates and eigensolutions are, in fact, significantly different from those derived on the basis of 'low-β' model configurations that omit one or both of the effects mentioned above, and provide different indications for the expected interaction between ideal-MHD and kinetic modes. For each value of the shear parameter $\hat{s}$, the normalized growth rate Γ becomes real at a critical value of the dimensionless pressure gradient parameter G. When the latter is increased at constant $\hat{s}$, Γ is found to increase only up to a saturation point, after which it decreases and tends to vanish at a second critical value of G.

1. INTRODUCTION

A major question concerning any magnetic confinement configuration is the maximum plasma pressure that it can sustain. This is a rather complex problem, as for different values of β (the ratio β of the kinetic to the magnetic pressure) different transport processes and instabilities can be excited. In general, there are no values of β for which no collective modes are present.

Here we limit our consideration to the ideal-MHD approximation for which the plasma is constrained to move with the magnetic field lines, and we investigate the stability properties of ballooning modes for increasing values of β. These modes have amplitudes that vary along a given magnetic field line and have their maximum at the points where the influence of the local magnetic field curvature is most unfavourable to mode stability [1–4].

The onset of the relevant instability is, in fact, related to the dimensionless parameter

$$\hat{\beta} = \beta L^2/(4\pi^2 r_p R_c) \qquad (1.1)$$

where L is the so-called connection length characterizing the modulation of the magnetic field intensity along a given line of force, R_c is the minimum radius of curvature, and

$$r_p = p/|\nabla p| \qquad (1.2)$$

is the pressure gradient scale distance. When the parameter $\hat{\beta}$ is of order unity the model equilibrium configurations that can be adopted to study the onset of ideal-MHD ballooning modes can no longer be as simple as those adopted to study other types of modes such as those involving trapped-particle or resistive effects. The latter type of mode can, in fact, be excited and be adequately studied in model configurations where $\hat{\beta} < 1$ and where the magnetic surfaces can be assumed to be toroids with circular and concentric cross-sections.

In particular [5, 6], when $\hat{\beta} \sim 1$, the poloidal magnetic field has a significant variation, as a function of the poloidal angle, on a given magnetic surface. In addition, the rate of magnetic shear also acquires a strong dependence on the poloidal angle. The same can be said about the scale distance r_p. Therefore, we can expect to find a stability criterion, for ideal-MHD ballooning modes, of the form $\hat{\beta} = \hat{\beta}_c$ where $\hat{\beta}_c$ is finite and, like L and r_p, is a function of β. Thus no simple expression for the critical β can be given.

The analytical studies of ballooning-mode stability which have been produced so far have concentrated largely on questions connected with their topology and their representation. Therefore, these studies have been carried out on simplified model configurations that are either adequate for cases where $\hat{\beta} < 1$ or do not contain most of the important factors that characterize a configuration with $\hat{\beta}$ finite.

* On leave from the Instituto de Energia Atômica, São Paulo, Brasil.

We observe that the characteristics of confinement configurations that are to be obtained experimentally will depend on the adopted heating cycle to the extent that they can achieve finite $\hat{\beta}$ values through magnetic-flux conservation.

In the present paper, we have made an attempt to evaluate the stability properties of ballooning modes for finite values of $\hat{\beta}$ on the basis of model equations which include, at the same time, the modulation of the normal and geodesic magnetic curvatures, of the poloidal field and of the rate of magnetic shear. We find that the relevant growth rates are significantly different and, in fact, lower than those evaluated from more simplified model configurations, and, to the extent that the types of assumed model equation are valid, they tend to vanish, for sufficiently large values of $\hat{\beta}$.

One of the main reasons for our study, besides that of explaining and complementing the result of existing sophisticated numerical codes, is to formulate analytical models on the basis of which the influence of various types of kinetic effects such as finite drift wave frequency, finite Larmor radius, trapped particles, etc. could be investigated later. It is, in fact, important to evaluate the effects of the interaction between ideal-MHD ballooning modes and other modes such as the resistive ballooning mode or the ubiquitous mode which do not involve the constraint that the plasma move with the magnetic field lines.

This paper is organized as follows:

In Section 2, we introduce the basic partial differential equation describing the most unstable ballooning modes. This eigenvalue equation for the growth rate was derived from the linearized MHD equations in the high-mode-number limit [7–9]. For our present application, this equation reduces to an ordinary differential equation if we either adopt the so-called 'disconnected-mode approximation' [4] or if we adopt an infinite-series representation for the relevant plasma displacement [10, 11].

In Section 3, the same equation is expressed in a more general non-orthogonal co-ordinate system, with no constraint on the definition of the poloidal co-ordinate. This allows us to continue to use a geometrical poloidal angle as a co-ordinate, even though the relevant flux surfaces are not concentric.

Section 4 is devoted to the 'finite-β' equilibrium model that provides the simplest basis for our study of the ballooning-mode instability. It includes most of the important physical effects described above. This configuration is one where the magnetic surfaces are circular non-concentric toroids [12]. The important features of this model are a significant dependence of the poloidal field and the local shear on the poloidal angle. When these effects are taken into account it is clear from mere inspection of the differential equation or its associated quadratic form that the growth rate does not follow the 'low-β' behaviour characteristic of equilibria with concentric circular magnetic surfaces. Specifically, the squared growth rate Γ^2 is no longer a linear function of the pressure gradient parameter, $G = -8\pi\, q^2 R_0 B_0^{-2}\, dp/dr$.

Section 5 displays the values of Γ as a function of G for given values of the shear parameter $\hat{s} = d \ln q/d \ln r$. These Γ-values are obtained from our model equation either by means of the variational method or by numerical solution of the appropriate differential equation. In the solution of this differential equation, we have used both the boundary conditions relevant to the 'disconnected-mode' [4] and the 'infinite-domain' [10, 11] approaches. These boundary conditions give the same qualitative results. Quite close quantitative agreement also occurs in the most important ranges of the relevant parameters. A detailed comparison with simpler model configurations is also given.

2. THE BASIC EQUATIONS

In toroidal plasma columns with no equilibrium macroscopic flows, we consider linear perturbations to the ideal-MHD set of equations,

$$\rho \frac{d\vec{v}}{dt} = -\nabla p - \frac{1}{c}\vec{J} \times \vec{B} \tag{2.1}$$

$$\frac{\partial \rho}{\partial t} + \nabla \cdot (\rho \vec{v}) = 0 \tag{2.2}$$

$$\frac{\partial \vec{B}}{\partial t} = \nabla \times (\vec{v} \times \vec{B}) \tag{2.3}$$

$$\vec{J} = \frac{c}{4\pi} \nabla \times \vec{B} \tag{2.4}$$

$$\nabla \cdot \vec{B} = 0 \tag{2.5}$$

$$\frac{d}{dt}(p/\rho^{\gamma}) = 0 \tag{2.6}$$

If we consider axisymmetric configurations, perturbed quantities such as the plasma displacement $\vec{\xi}(\vec{x}, t)$ can be represented by normal-mode solutions of the form

$$\vec{\xi}(\vec{x},t) = \vec{\xi}(\chi,\psi)\ \exp\left\{ - i\omega t \right.$$

$$\left. + i\, n^{o}\left[\zeta - \int^{\chi} \nu(\psi,\chi')\, d\chi'\right]\right\} \qquad (2.7)$$

where (ψ, χ, ζ) are the usual orthogonal curvilinear co-ordinates with magnetic surfaces given by ψ = constant, and with χ, ζ in the poloidal and toroidal directions. These co-ordinates have corresponding scale factors:

$$h_{\psi} = \frac{1}{RB_p} \quad , \quad h_{\chi} = B_p J_o \quad , \quad h_{\zeta} = R \qquad (2.8)$$

where R is the cylindrical radial distance from the symmetry axis of the toroid, B_p is the magnitude of the poloidal field and J_0 is the Jacobian

$$J_o = \left| \frac{\partial(x,y,z)}{\partial(\psi,\chi,\zeta)} \right| \qquad (2.9)$$

The function $\nu(\psi, \chi)$ is defined by

$$\nu(\psi,\chi) = d\zeta/d\chi \quad \begin{matrix}(\text{along a given} \\ \text{magnetic field line})\end{matrix} \qquad (2.10)$$

and the range of variation for χ is chosen to be $[-\pi, \pi]$.

The scale distance between adjacent mode rational surfaces is

$$r_q = q/(n^{o}|\nabla q|) \qquad (2.11)$$

where q stands for the inverse rotational transform,

$$q(\psi) = (2\pi)^{-1} \oint \nu(\psi,\chi) d\chi \qquad (2.12)$$

Since we are interested in determining the conditions of marginal stability rather than in evaluating the magnitude of the growth rate, we shall consider plasma displacements subject to the constraint:

$$\vec{B} \cdot \nabla \times (\vec{\xi} \times \vec{B}) - 4\pi \vec{\xi} \cdot \nabla p = 0 \qquad (2.13)$$

which is a sufficient condition to avoid the fast magneto-sonic mode and is satisfied by marginally stable modes in the limit $r_q < r_p$. In this limit, following the procedure indicated in Ref. [7], we obtain:

$$- \frac{\omega^2}{v_A^2} \left\{ 1 + \sigma^2 \left(\Theta + i \frac{\partial}{\partial S}\right)^2 \right\} T(\chi,S)$$

$$= \frac{h_{\chi}}{Rv^2 h_{\psi}} \frac{\partial}{\partial \chi} \left\{ \frac{h_{\psi}}{Rh_{\chi}} \left[1 + \sigma^2 \left(\Theta + i \frac{\partial}{\partial S}\right)^2 \right] \frac{\partial T}{\partial \chi} \right\}$$

$$- \frac{8\pi}{h_{\psi} B^2} \frac{dp}{d\psi} \left[- \kappa_{\psi} + \kappa_{\chi} \sigma \left(\Theta + i \frac{\partial}{\partial S}\right) \right] T \qquad (2.14)$$

Here $T(S, \chi)$ is related to the 'radial' plasma displacement ξ_{ψ} by

$$T(S,\chi) = \hat{\xi}_{\psi}/h_{\psi} \qquad (2.15)$$

In the considered limit ($r_q < r_p$), the displacement depends on the flux co-ordinate only through the fast variable [7] $S = n^0 q(\psi)$; the co-ordinate ψ is regarded as a parameter when it appears in the slowly varying equilibrium quantities that are involved in the coefficient functions of the differential equation (2.14). The functions σ and Θ are defined by

$$\sigma = \frac{h_{\chi}}{h_{\psi}} \frac{1}{\nu} \frac{dq}{d\psi} \qquad (2.16)$$

$$\Theta = \int^{\chi} \frac{d\nu/d\psi}{dq/d\psi} d\chi' \qquad (2.17)$$

v_A is the Alfvén speed [$v_A^2 = B^2/(4\pi\rho)$] and κ_{ψ}, κ_{χ} are the two components of the curvature vector $B^{-2}(\vec{B}\cdot\nabla)\vec{B}$, perpendicular to $\vec{B}$. In Ref. [7], the basic analysis for studying ballooning modes has been outlined. There, the general properties of the partial differential equation (2.14) in (S, χ) have been described, particularly for the case of concentric circular magnetic surfaces (i.e. low-β plasmas). In particular, we may adopt the disconnected-mode approximation [4] that leads to the ordinary differential equation

$$- \frac{\omega^2}{v_A^2} \left\{ 1 + \sigma^2\, \Theta^2(\chi) \right\} T(\chi)$$

$$= \frac{h_{\chi}}{Rv^2 h_{\psi}} \frac{\partial}{\partial \chi} \left\{ \frac{h_{\psi}}{Rh_{\chi}} \left[1 + \sigma^2\, \Theta^2\,(\chi) \right] \frac{\partial T(\chi)}{\partial \chi} \right\}$$

$$- \frac{8\pi}{h_{\psi} B^2} \frac{dp}{d\psi} \left[- \kappa_{\psi} + \kappa_{\chi} \sigma\, \Theta\,(\chi) \right] T\,(\chi) \qquad (2.18)$$

in the interval $-\pi < \chi < \pi$ subject to the boundary conditions

$$T(\pm\pi) = 0 \qquad (2.19)$$

This approximation is suitable in the physically interesting limit where the S-dependence of Υ can be neglected over most of the interval $[-\pi, \pi]$, and where the mode amplitude is sharply peaked around $\chi = 0$ as in the case of growing ballooning modes.

We can be led to solve the same one-dimensional equation by adopting the representation for Υ outlined in the Appendix, and proposed previously by several authors [10, 11]. In this case the appropriate boundary conditions are

$$T(\pm \infty) = 0 \tag{2.20}$$

These approaches give qualitatively the same physical conclusions (see Section 5), with quantitive difference mostly when there is small shear in the magnetic field, and the disconnected-mode approximation is by definition not appropriate.

3. A GENERAL CHANGE OF CO-ORDINATES

It is physically convenient to transform Eq. (2.18) and write it in terms of new variables (r, θ) where

$$r = r(\psi) \quad , \quad \theta = \theta(\psi, \chi) \tag{3.1}$$

In Section 4, the variables r and θ will actually be identified as the radius and poloidal angle in a system of co-ordinates corresponding to magnetic surfaces which are displaced circles.

Defining the Jacobian

$$J = \left| \frac{\partial (x,y,z)}{\partial (r,\theta,\zeta)} \right| \tag{3.2}$$

we note that

$$\frac{1}{J_o} \left(\frac{\partial f}{\partial \chi} \right)_\psi = \frac{d\psi}{dr} \frac{1}{J} \left(\frac{\partial f}{\partial \theta} \right)_r \tag{3.3}$$

Thus the quantity $\nu(\psi, \chi)$ of Eq. (2.10) can be written in terms of

$$q_\ell(r,\theta) = d\zeta/d\theta \quad \begin{matrix} \text{(along a magnetic} \\ \text{field line)} \end{matrix} \tag{3.4}$$

by means of the relation

$$\nu = \frac{J_o}{J} \frac{d\psi}{dr} q_\ell \tag{3.5}$$

From this equation and Eq. (2.8)

$$\frac{h_\chi}{\nu} = \frac{JB_p}{q_\ell (d\psi/dr)} \tag{3.6}$$

Another important quantity in Eq. (2.18) is

$$\Sigma \equiv \sigma \Theta = \frac{h_\chi}{h_\psi} \frac{1}{\nu} \frac{\partial}{\partial \psi} \int^\chi \nu \, d\chi'$$

$$= \frac{JRB_p^2}{q_\ell (d\psi/dr)^2} \left[\frac{\partial}{\partial r} + \frac{\nabla\theta . \nabla r}{|\nabla r|^2} \frac{\partial}{\partial \theta} \right] \int^\theta q_\ell \, d\theta' \tag{3.7}$$

where $(\nabla\theta . \nabla r / |\nabla r|^2)$ depends on the exact nature of the transformation (3.1).

Let us also define

$$G(r) = - \frac{8\pi R_o r^2}{(d\psi/dr)} \frac{dp}{d\psi} \tag{3.8}$$

$$\Gamma^2(r) = - \frac{\omega^2 B^2 R_o^2 r^2}{v_A^2 (d\psi/dr)^2} \tag{3.9}$$

where $R = R_0$ is the radial distance of the magnetic axis. Then from the use of Eqs (3.2) to (3.9), the fundamental Eq. (2.18) can be transformed into

$$\Gamma^2 (1 + \Sigma^2) T = \frac{B^2 J B_p^2 R_o^2 r^2}{q_\ell^2 (d\psi/dr)^2} \frac{\partial}{\partial \theta} \left\{ \frac{1}{R^2 B_p^2 J} (1+\Sigma^2) \frac{\partial T}{\partial \theta} \right\}$$

$$+ \frac{GR_o B_p}{(d\psi/dr)} \left[- R\kappa_\psi + R\kappa_\chi \Sigma \right] T \tag{3.10}$$

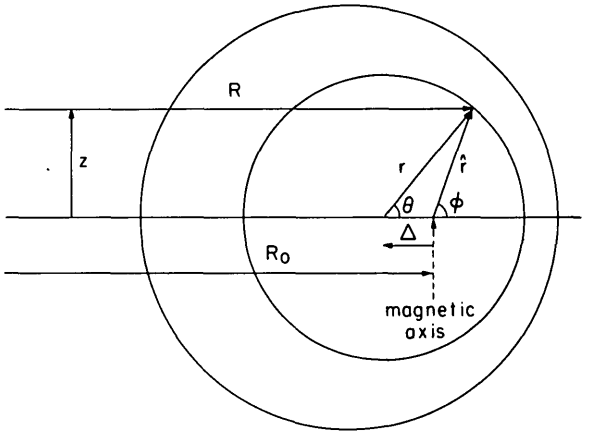

FIG.1. Co-ordinate system adopted.

At this point it is convenient to derive, from Eq. (3.10), the following quadratic form:

$$r^2 \mathcal{J}_I = \mathcal{J}_c - \mathcal{J}_A \tag{3.11}$$

where

$$\mathcal{J}_I = \int \frac{(d\psi/dr)^2 q_\ell^2}{B_p^2 R_o^2 B^2 r^2 J} (1 + \Sigma^2) T^2 \, d\theta \tag{3.12}$$

$$\mathcal{J}_c = \int \frac{d\psi/dr \, q_\ell^2 G}{B_p R_o B^2 r^2 J} (- R \kappa_\psi + R \kappa_x \Sigma) T^2 \, d\theta \tag{3.13}$$

$$\mathcal{J}_A = \int (R^2 B_p^2 J)^{-1} (1 + \Sigma^2) \left(\frac{\partial T}{\partial \theta} \right)^2 d\theta \tag{3.14}$$

are, respectively, the inertial, curvature and shear-Alfvén terms.

4. DISPLACED CIRCULAR MAGNETIC SURFACES

In this section, we consider for simplicity the configuration in which magnetic surfaces are represented as displaced circles. We find that this representation already incorporates some of the most important effects of 'finite-β' equilibria. Thus we write [12]:

$$R = R_o + \Delta(r) + r \cos\theta$$

$$z = r \sin\theta \tag{4.1}$$

where r is the radius of the circular magnetic surface whose centre is displaced by the distance $\Delta(r)$ from the magnetic axis at $R = R_o$ (Fig. 1). The angle θ is the usual poloidal angle referred to the centre of this circle. By our definition, and the knowledge of such equilibria [12], we know that

$$\Delta < 0, \qquad d\Delta/dr < 0 \tag{4.2}$$

It is straightforward to show that

$$RB_p = | \nabla\psi | = \frac{d\psi/dr}{1 - \alpha_\theta \cos\theta} \tag{4.3}$$

where

$$\alpha_\theta(r) \equiv - d\Delta(r)/dr \tag{4.4}$$

and

$$J = Rr(1 - \alpha_\theta \cos\theta) \tag{4.5}$$

$$JB_p = r \, d\psi/dr \tag{4.6}$$

$$\frac{\nabla_\theta \cdot \nabla r}{|\nabla r|^2} = - \frac{1}{r} \frac{d\Delta}{dr} \sin\theta \tag{4.7}$$

We shall assume a large aspect ratio and neglect the variation of R, $R \cong R_o$; similarly, the toroidal field will be assumed to be constant over the plasma region. However, the variation of the poloidal field with θ, characteristic of finite-β configurations, will be retained. This means that we are assuming r/R_o and Δ/R_o to be negligible as compared to unity, but $d\Delta/dr$ can be comparable to one.

We can now express the quantity q_ℓ of Eq. (3.4) as

$$q_\ell (r,\theta) = \frac{B_T r}{B_p R} \simeq q(r) \, (1 - \alpha_\theta \cos\theta) \tag{4.8}$$

$$q(r) = B_T \, r \, (d\psi/dr)^{-1} \tag{4.9}$$

In Eq. (3.7) the expression Σ can be written as

$$\Sigma = \frac{\hat{s}\theta - \alpha_q \sin\theta + \frac{1}{2}\alpha_\theta^2 \sin 2\theta}{(1 - \alpha_\theta \cos\theta)^2} \tag{4.10}$$

where we have used Eqs (4.3) and (4.6) to (4.8), and defined

$$\alpha_q \equiv \alpha_\theta \left[1 + \hat{s} + \frac{d\ln\alpha_\theta}{d\ln r} \right] \tag{4.11}$$

$\hat{s}$ being the usual shear parameter

$$\hat{s} = \frac{d\ln q}{d\ln r} \tag{4.12}$$

Equation (3.10) can now be rewritten as

$$r^2(1+\Sigma^2)T = \left(\frac{q}{q_\ell} \right)^3 \frac{\partial}{\partial\theta} \left\{ \left(\frac{q_\ell}{q} \right) (1+\Sigma^2) \frac{\partial T}{\partial\theta} \right\} + G \left(\frac{q}{q_\ell} \right) [\cos\theta + \sin\theta \Sigma] T \tag{4.13}$$

with G, Γ, (q/qℓ), Σ defined in Eqs (3.8), (3.9), (4.8), (4.10), respectively.

The quantities α_θ, α_q and G are related to each other, and a detailed solution of the equilibrium problem is needed to obtain this relationship. In the present work, we shall adopt two simple representations for α_θ and α_q:

$$\alpha_\theta \simeq G/4 \tag{4.14}$$

$$\alpha_q \simeq (2+\hat{s})\alpha_\theta \tag{4.15}$$

To derive Eqs (4.14) and (4.15), we write Grad-Shafranov's equation in our co-ordinate system (4.1), assuming ψ to be a function of r only. This equilibrium equation is then expanded in powers of r about the magnetic axis. Up to linear terms, it yields:

$$(\psi'' + \psi'/r) - [2\Delta'\psi'' + (\Delta' + r\Delta'')\psi'/r]\cos\theta = (4\pi/c)R_0 j(0) - 8\pi R_0 r p_\psi(0)\cos\theta \tag{4.16}$$

where primes denote differentiation with respect to r, and j(0) and $p_\psi(0)$ are, respectively, the current density and the derivative of the pressure with respect to ψ at the magnetic axis. The quantities r/R_0 and Δ/R_0 have again been neglected as compared to Δ'.

The characteristic equilibrium parameter

$$\lambda = -2cR_0 p_\psi(0)/j(0) \tag{4.17}$$

scales like β_p, the poloidal beta, and, therefore, finite-β configurations are characterized by values of λ of the order of the aspect ratio. We note that this fact is still compatible with the analytical representation of the flux surfaces as shifted circles, which remains accurate to the extent that $\epsilon\beta_p \lesssim 1$, ϵ being the inverse aspect ratio. This ordering for λ implies that the two terms on the right-hand side of Eq. (4.16) are comparable and that Δ' is of order unity. Specifically, from Eq. (4.16) we obtain

$$\psi = (\pi/c)\, R_0 j(0) r^2 \tag{4.18}$$

$$\Delta' = -\lambda r/(2R_0) \tag{4.19}$$

Recalling the definition of G, Eq. (3.18), we can now write the first term of its expansion in powers of r:

$$G = 2\lambda r/R_0 \tag{4.20}$$

From Eqs (4.19), (4.20), (4.4) and (4.11) we readily obtain the representations (4.14, 15) for α_θ and α_q.

The previous derivation shows that Eqs (4.14, 15) are strictly valid for finite-β configurations in the vicinity of the magnetic axis, where both G(r) and $\alpha_\theta(r)$ increase linearly with r. Most important, they provide a model for the physically relevant non-linear dependence of the coefficient functions in Eq. (4.13) on the parameter G, thus allowing some of the finite-β effects to be included in the mode stability analysis.

5. GROWTH RATES AND EIGENSOLUTIONS IN DIFFERENT MODEL CONFIGURATIONS

Now we examine the solutions of the differential equation (4.13) under the two boundary conditions (2.19) and (2.20), using a range of values of the equilibrium parameters G, $\hat{s}$, $\alpha_\theta(G)$, $\alpha_q(G)$ of Eqs (3.8), (4.12), (4.14), and (4.15). We are interested in the lowest even eigenfunction, which is the one that evolves at the highest growth rate and determines the strictest conditions for marginal stability.

A. The $\alpha_\theta = \alpha_q = 0$ case

This is the classical case which, as is well known [5, 6], is not applicable to finite-β equilibria, but is interesting in order to illuminate our new results for the dimensionless growth rate Γ as a function of the pressure gradient parameter G.

The choice $\alpha_\theta = 0$, $\alpha_q = 0$ corresponds to a nearly pressureless toroidal plasma, where the flux surfaces are concentric circles. The relevant differential equation takes the form

$$\frac{d}{d\theta}\left[(1+\hat{s}^2\theta^2)\frac{dT}{d\theta}\right] + G(\cos\theta + \hat{s}\sin\theta)\,T = \Gamma^2(1+\hat{s}^2\theta^2)T \tag{5.1}$$

For the case in which $\hat{s} \ll 1$, the above equation reduces to

$$\frac{d^2T}{d\theta^2} + G\cos\theta T = \Gamma^2 T \tag{5.2}$$

In the limit $G > 1$, the lowest eigensolution is well represented by a Gaussian function

$$T = \exp\left[-1/2\ \theta^2\ (G/2)^{1/2}\right] \tag{5.3}$$

and, correspondingly, the eigenvalue is given approximately by

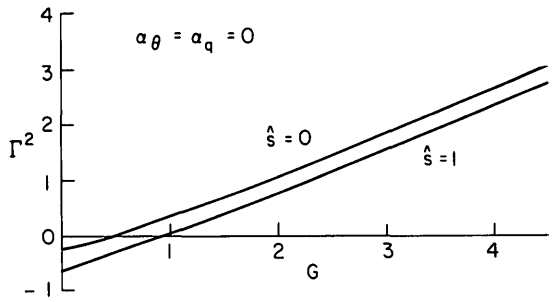

FIG.2. Non-dimensional squared growth rate Γ^2 as a function of pressure gradient parameter G in a low-β model configuration for two fixed values of the magnetic shear parameter $\hat{s}$.

$$\Gamma^2 \simeq G - (G/2)^{1/2} \qquad (5.4)$$

On the basis of Eq. (5.4), which predicts that the mode becomes more unstable as the stability parameter G is increased, we expect the occurrence of only one point of marginal stability. This fact is illustrated in Fig. 2, where the squared growth-rate Γ^2 obtained numerically from Eq. (4.13) was plotted as a function of G for several values of the shear parameter $\hat{s}$ (the boundary condition $\Upsilon(\pi) = 0$ was applied).

Even though the simple analytical representation (5.3) cannot be extended to more general conditions of equilibrium, it will remain true that strongly unstable modes tend to the localized in the vicinity of the outer edge of the plasma column ($\theta \approx 0$). However, the qualitative behaviour of Eq.(4.13) when α_θ and α_q are non-vanishing differs from the result given in Fig. 2 for large G ($G > 1$). In fact, a simple asymptotic discussion shows that, for α_θ increasing monotonically with G, Eq. (4.13) does not allow localized solutions with $\Gamma^2 > 0$ when G is very large. A more detailed discussion follows in the next subsection.

B. Results from the finite-β model equation

Here we are reporting the results of the numerical solution to our model equation (4.13) in order to get the square Γ^2 of the normalized growth rate (Eq. (3.9)) as a function of the parameters G(Eq. (3.8)) and $\hat{s}$ (Eq. (4.12)). The obtained eigenvalues Γ^2 correspond to the most unstable (no nodes) eigensolutions subject to the relevant boundary conditions (2.19) and (2.20). In the coefficient functions of the differential equation, we have chosen the representations (4.14) and (4.15) for α_θ and α_q, and dropped the $\alpha_\theta^2 \sin 2\theta$ term in Σ (Eq. (4.10)); as a matter of fact, the inclusion of this term only amounts to small quantitative changes at large values of G, where the assumed proportionality between α_θ and G is not expected to be accurate anyway. For any fixed G and $\hat{s}$, Eq. (4.13) was integrated by finite differences with initial conditions $\Upsilon(0) = 1$, $\Upsilon'(0) = 0$; the eigenvalue Γ^2 was varied until the first eigensolution satisfying the boundary condition $\Upsilon(\pi) = 0$ or $\Upsilon(N\pi) = 0$ ($N \to \infty$) was found. For the boundary problem (2.20) only positive values of Γ^2 were sought, because when $\Gamma^2 < 0$, both independent solutions to the differential equation tend to zero as $|\theta| \to \infty$.

Figure 3 gives the lowest-mode growth rate Γ^2 as a function of G for several fixed values of $\hat{s}$, and for the two different boundary conditions. Based on our present model, the major conclusion is that the increase of the growth rate is limited and the lowest mode stabilizes again for large enough values of G. Within the limits ($G < 4$) where this model can be applied, we have found numerically that all higher eigensolutions are stable. These results are summarized in Fig. 4, where we plot the marginal stability curves corresponding to the two boundary conditions; the shaded region indicates instability.

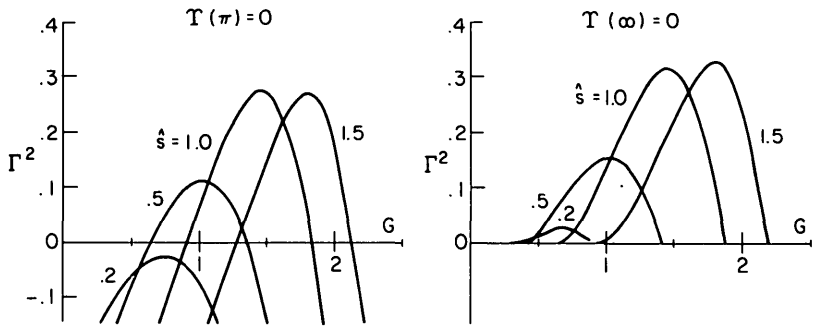

FIG.3. Eigenvalue Γ^2 for a finite-β model configuration obtained from numerical solution of Eq. (4.13), as a function of G. The two sets of curves correspond to the use of boundary conditions (2.19) and (2.20) at various fixed values of $\hat{s} = d \ln q / d \ln r$.

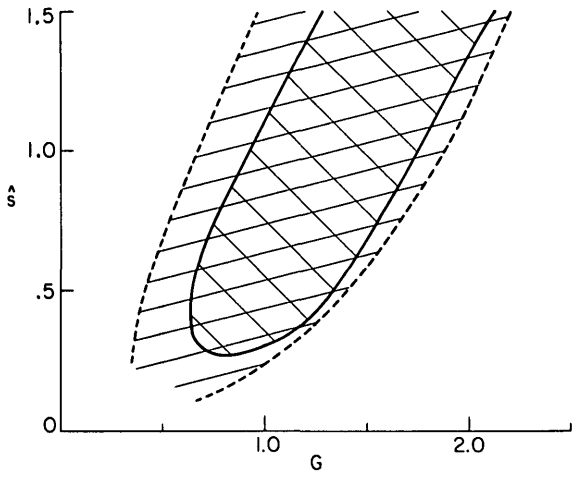

FIG.4. Marginal stability curves in the finite-β model configuration. The shaded region corresponds to instability. The solid curve was obtained with the disconnected-mode boundary conditions (2.19) while the broken ones were obtained with boundary conditions (2.20).

A few of the relevant eigenfunctions are given in Fig. 5 for $\hat{s} = 1$. We emphasize that, even for the second marginal stability point, we are indeed evaluating the most unstable eigenfunction which has no nodes. For marginal stability, the boundary condition (2.20) results in eigensolutions with very slow decay as $|\theta| \to \infty$. Of course, the numerical solution is difficult to obtain for this latter $\Gamma^2 = 0$ case because of that slow convergence. But for Γ^2 positive (even though small, as for a case $\hat{s} = 1$, $G = 1.87$, $\Gamma^2 = 0.008$ which we evaluated) and $\hat{s} \sim 1$ or larger, the exponential decay dominates the large $-|\theta|$ behaviour.

We note that the most unstable ($\hat{s} \sim 1$) solutions do not show much difference between the boundary conditions (2.19) and (2.20). For low values of $\hat{s}$, where the disconnected-mode approximation tends to break down completely, the direct two-dimensional representation described in Ref. [7] and the associated quadratic form are to be used for a more meaningful comparison with the results of the infinite-series representation.

C. Discussion on the basis of the quadratic form

The interesting dependence of the squared growth rate Γ^2 on the pressure gradient parameter G, discussed in the previous section, is due to a combination of competing physical effects. Their respective contributions to Eq. (4.13) are more apparent if we consider the associated quadratic form

$$\Gamma^2 = \frac{\mathcal{J}_C - \mathcal{J}_A}{\mathcal{J}_I} \tag{5.5}$$

where

$$\mathcal{J}_C = G \int (1-\alpha_\theta \cos\theta)^2 [\cos\theta + \sin\theta \frac{\hat{s}\theta - \alpha_q \sin\theta}{(1-\alpha_\theta\cos\theta)^2}] T^2 \, d\theta \tag{5.6}$$

represents the effects of magnetic curvature,

$$\mathcal{J}_A = \int (1-\alpha_\theta\cos\theta)\left[1 + \frac{(\hat{s}\theta - \alpha_q \sin\theta)^2}{(1-\alpha_\theta\cos\theta)^4}\right]\left(\frac{dT}{d\theta}\right)^2 d\theta \tag{5.7}$$

is related to the restraining effect of the shear-Alfvén perturbation of the field lines, and finally the inertial effects are associated with the term

$$\mathcal{J}_I = \int (1-\alpha_\theta\cos\theta)^3 \left[1 + \frac{(\hat{s}\theta - \alpha_q \sin\theta)^2}{(1-\alpha_\theta\cos\theta)^4}\right] T^2 d\theta \tag{5.8}$$

We have on purpose exhibited all dependences on α_θ and α_q which according to Eqs (3.14) and (3.15) are linear functions of G, within our approximations.

It is well known that the Alfvén term $\mathcal{J}_A$ is stabilizing while the curvature term $\mathcal{J}_C$ is mostly de-stabilizing. But the net result of increasing values of β is a general stabilizing tendency in the three terms. We illustrate this in Fig. 6, where we plot $\mathcal{J}_C, \mathcal{J}_A, \mathcal{J}_I$ and also Γ^2 as functions of G, evaluated at $\hat{s} = 1$, using the trial function

$$T_T(\theta) = C(1+\cos\theta) \tag{5.9}$$

where C is a normalization constant. This function is even in θ and satisfies the boundary condition (2.19). Note that it gives reasonable values for the marginal stability points where $\Gamma^2 = 0$ (Fig. 3); it does not do quite so well for the max (Γ^2).

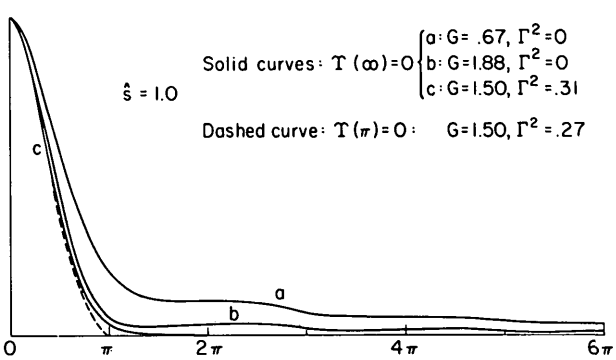

FIG.5. Amplitudes for a sample of eigenfunctions in our finite-β model configuration at shear parameter ŝ = 1.

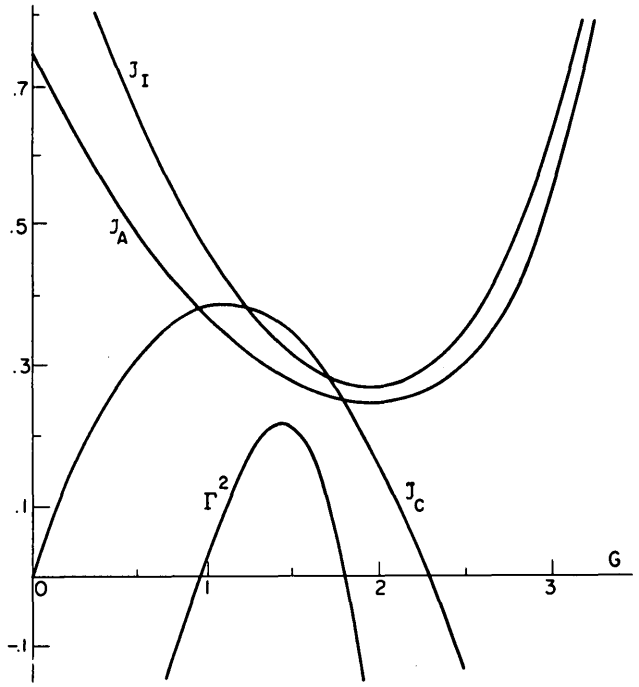

FIG.6. Representation as functions of G, for $\hat{s} = 1$, of the terms entering the quadratic form (5.5).

Detailed examination of the numerical results of Section (5.B) as well as of Eqs (5.5) to (5.8) shows that a substantial stabilizing influence can be attributed to the α_θ-term due to the finite variation of the poloidal field on a magnetic surface. The qualitative behaviour of Figs 3 and 4 can be reproduced by a simpler though not necessarily self-consistent model where we somehow imagine that in Eq. (4.14)

$$\alpha_\theta \sim 0 \tag{5.10}$$

but retain the effect of non-uniform shear on a magnetic surface,

$$\hat{\alpha}_q \equiv \alpha_q/G \simeq (2+\hat{s})/4 \neq 0 \tag{5.11}$$

Note that since for $\hat{s} \sim 1$ the second marginal point of Fig. 3 is at $G \sim 2$, where $\alpha_\theta \sim 1/2$, the neglect of α_θ is difficult to justify. But if we do neglect it, the advantage is that Eqs (5.6) to (5.8) can be reduced to the simple analytical expressions

$$\mathcal{J}_C \sim \frac{\pi}{4}\left[-\frac{5}{4}\hat{\alpha}_q G^2 + \left(2 + \frac{5}{3}\hat{s}\right) G \right] \tag{5.12}$$

$$\mathcal{J}_A \sim \frac{\pi}{4}\left\{ \frac{3}{4}\hat{\alpha}_q{}^2 G^2 - \frac{8}{3}\hat{s}\hat{\alpha}_q G + \left[\hat{s}^2\left(\frac{\pi^2}{3} - \frac{1}{2}\right) + 1 \right] \right\} \tag{5.13}$$

and

$$\mathcal{J}_I \sim \frac{\pi}{4}\left\{ \frac{5}{4}\hat{\alpha}_q{}^2 G^2 - \frac{10}{3}\hat{s}\hat{\alpha}_q G + \left[\hat{s}^2\left(\pi^2 - \frac{15}{2}\right) + 3 \right] \right\} \tag{5.14}$$

which exhibit quadratic behaviour in G reminiscent of the results of Fig. 6. However, a comparison between the quantitative estimates provided by Eqs (5.12)–(5.14) and those displayed in Fig. 6 shows that the size of the unstable region in Fig. 4 and the maximum growth rate in Fig. 3 would be overestimated if α_θ were omitted.

CONCLUDING REMARKS

We have seen that the stability of ballooning modes depends on the finite-β aspects of the equilibrium configuration. The normal-mode differential equation depends non-linearly on the pressure gradient parameter G, reflecting the dual role that G plays in the stability problem. On the one hand, G accounts for the de-stabilizing effect of the pressure gradient through the curvature of magnetic field lines; on the other hand, it represents a measure of the shortening of the connection length, which has a stabilizing effect on finite-β configurations. The net result is the appearance of a second stable region in the G-$\hat{s}$ plane.

To obtain this result, a simple model which encompasses some of the relevant finite-β effects, was used. This model is accurate in the neighbourhood of the magnetic axis where both G and $\hat{s}$ are small. Within its expected range of validity, it predicts two branches of marginally stable points. Thus there is no doubt about the existence of a second curve of marginal stability in the G-$\hat{s}$ plane, although its exact location may differ from our estimates when G or $\hat{s}$ become large.

The important issue is now whether it is possible to reach the second stable region with realistic high-β equilibria. In the present treatment, we have considered G and $\hat{s}$ as independent variables, and this is appropriate in order to carry out a local stability analysis that can be applied to a variety of equilibrium configurations. However, for a given configuration, G and $\hat{s}$ are not independent as they both are functions of the flux coordinate only. Therefore, the physical relevance of the second stability region will depend upon the possibility of realizing a sequence of stable equilibria whose G-$\hat{s}$ points lie within that region. Preliminary results obtained by some of us [13], on the basis of numerical high-β flux-

conserving equilibria with conducting plasma boundary, suggest that consistent sets of values for G and $\hat{s}$, lying in the second stable region, can be produced.

ACKNOWLEDGEMENTS

It is a pleasure to thank S. Migliuolo and T. Antonsen for their derivation of Eq. (2.14), and J. Cordey and J. Wesson for a series of conversations during the 1977 Varenna School on the topics treated by this paper.

This work was supported in part by the US Department of Energy.

One of us (A.F.) is indebted to Fundacão de Amparo a Pesquisa do Estado de São Paulo, Brasil, for a fellowship; J.J.R. was partially supported by a PFPI (MEC Spain) grant.

Appendix
'INFINITE-DOMAIN' REPRESENTATION FOR Υ

In this Appendix, we justify the use of the ordinary differential equation (2.18) in the infinite domain $[-\infty, \infty]$ for the independent variable $\hat{\chi}$.

In the system of co-ordinates used in Section 2, χ represents the poloidal variable, so that physical quantities are periodic over its specified range $\Delta\chi = 2\pi$. Included among such physical variables which are periodic in χ, we may specially consider

$$\Xi(S,\chi) \equiv \Upsilon(S,\chi)\exp\{-in^0\int^{\chi}\nu(\chi')d\chi'\} \qquad (A.1)$$

For this quantity we have suppressed the slow dependence on the flux surface variable ψ and retained only the fast variable S defined in Section 2. Clearly, S is not involved in any of the coefficients of the partial differential equation (2.14). Therefore, we may choose solutions Υ which are periodic in S with period $\Delta S = 1$ and only parametrized by the slow variable ψ due to slow changes in equilibrium quantities (integer values of S correspond to mode rational surfaces; a more detailed discussion of the symmetries of this equation is given in Ref. [7]). Thus we write

$$\Upsilon(S,\chi)\exp\{in^0\int^{\chi}\nu d\chi'\}$$

$$= \sum_{m=-\infty}^{\infty} T_m(\chi)\exp\{-i[n^0\int^{\chi}\nu d\chi'+2\pi mS]\} \qquad (A.2)$$

Periodicity in χ implies that for all integers n,

$$\sum_{m=-\infty}^{\infty} T_m(\chi)\exp[-i2\pi mS]$$

$$= \sum_{m=-\infty}^{\infty} T_m(\chi+2\pi n)\exp\{-i2\pi(m+n)S\} \qquad (A.3)$$

Since this last expression for Υ must hold for all S, we must have

$$T_m(\chi) = T_{m-n}(\chi+2\pi n) \text{ for all } m,n$$

Alternatively,

$$T_m(\chi) = T_0(\chi + 2\pi m) \qquad (A.4)$$

so that

$$\Upsilon(S,\chi) = \sum_{m=-\infty}^{\infty} T_0(\chi+2\pi m)\exp(-i2\pi mS) \qquad (A.5)$$

Fourier-analysing Eq. (2.14) in terms of this periodicity in S, we obtain an ordinary differential equation involving χ-derivatives of $T_0(\chi+2\pi m)$ and where the term $[\Theta(\chi)+i\partial/\partial S]$ of Eq. (2.14) is replaced by $[\Theta(\chi)+2\pi m] \equiv \Theta(\chi+2\pi m)$. Defining the new variable

$$\hat{\chi} = \chi+2\pi m, \quad (-\infty<\hat{\chi}<\infty) \qquad (A.6)$$

we get Eq. (2.18) in the variable $(\hat{\chi})$:

$$-\frac{\omega^2}{v_A^2}\{1+\sigma^2\Theta^2(\chi)\}T_0(\hat{\chi})$$

$$= \frac{h_\chi}{R\nu^2 h_\psi}\frac{\partial}{\partial\hat{\chi}}\left\{\frac{h_\psi}{R h_\chi}\left[1+\sigma^2\Theta^2(\hat{\chi})\right]\frac{\partial T_0(\hat{\chi})}{\partial(\hat{\chi})}\right\}$$

$$-\frac{8\pi}{h_\psi B^2}\frac{dp}{d_\psi}[-\kappa_\psi+\kappa_\chi\sigma\Theta(\hat{\chi})]T_0(\hat{\chi}) \qquad (A.7)$$

In this equation, all other dependences on χ are periodic, so they may likewise be taken as periodic functions of $\hat{\chi}$, with the period equal to 2π, over the extended domain $-\infty<\hat{\chi}<\infty$. As is obvious from the above use of Fourier analysis, the boundary conditions which determine the eigenvalue ω^2 are

$$T_0(\hat{\chi}) \to 0 \qquad \text{as} \qquad |\hat{\chi}| \to \infty \qquad (A.8)$$

Of course, the mode structure in physical space requires the summing of the series (A.5), which is rather indirect

as well as giving rise to singularities in Υ at mode rational surfaces in the case of marginal stability [7].

However, for growing modes the disconnected-mode approximation [4] provides a more direct representation of the mode structure as well as giving numerical results quite close to Eq. (A.5). It was the first analytical approximation to the ballooning-mode problem. Within our recent line of derivation, the 'disconnected mode' also follows from Eq. (A.5) if we note that as $|\hat{\chi}| \to \infty$ or $|\theta| \to \infty$, the solution $\Upsilon(\hat{\chi})$ decays exponentially with exponent proportional to $|\omega\theta|$ due to the dominant θ^2 term of Eq. (2.14). Thus above marginal stability, the function $\Upsilon(\hat{\chi})$ is dominated by the $\hat{\chi} \sim 0$ or say $|\hat{\chi}| < \pi$ region, where $\Upsilon(\pm\pi)$ becomes negligible. In that case the sum (A.5) collapses to one term

$$\Upsilon(S,\chi) \simeq \Upsilon_0(\hat{\chi}) \qquad \text{(A.9)}$$

and $\Upsilon_0(\chi)$ can be obtained by solving Eq. (A.7) in the domain $-\pi < \chi = \chi < \pi$ with boundary conditions

$$\Upsilon_0(\pm\pi) = 0 \qquad \text{(A.10)}$$

NOTE ADDED IN PROOF

After this manuscript had been completed, we became aware of independent work on the second stability region, presented at the 1978 Innsbruck Conference [14–16]. More recently, the occurrence of the second stability region has been confirmed by numerical codes.

REFERENCES

[1] COPPI, B., ROSENBLUTH, M., in Plasma Physics and Controlled Nuclear Fusion Research 1965 (Proc. 2nd Int. Conf. Culham, 1965) Vol. 1, IAEA, Vienna (1966) 617.

[2] FURTH, H.P., KILLEEN, J.K., ROSENBLUTH, M.N., COPPI, B., ibid., 103.

[3] KULSRUD, R.M., ibid., 127.

[4] COPPI, B., Phys. Rev. Lett. **39** (1977) 939.

[5] COPPI, B., MARK, J.W.-K., FILREIS, J., FERREIRA, A., Bull. Am. Phys. Soc. **23** (1978) 606.

[6] COPPI, B., FILREIS, J., MARK, J.W.-K., in Plasma Physics and Controlled Nuclear Fusion Research (Proc. 7th Int. Conf. Innsbruck, 1978) Vol. 1, IAEA, Vienna (1979) 793.

[7] COPPI, B., FILREIS, J., PEGORARO, F., Analytical Representation and Physics of Ballooning Modes, Massachusetts Institute of Technology (RLE) Report PRR-78/22, Cambridge, Mass. (June 1978); to be published in Ann. Phys.

[8] DOBROTT, D., NELSON, D.B., GREENE, J.M., GLASSER, A.H., CHANCE, M.S., FRIEMAN, E.A., Phys. Rev. Lett. **39** (1977) 943.

[9] CHANCE, M.S., DEWAR, R.L., FRIEMAN, E.A., GLASSER, A.H., GREENE, J.M., GRIMM, R.C., JARDIN, S.C., JOHNSON, J.L., MANICKAM, J., OKABAYASHI, M., TODD, A.M.M., in Plasma Physics and Controlled Nuclear Fusion Research (Proc. 7th Int. Conf. Innsbruck, 1978) Vol. 1, IAEA, Vienna (1979) 686.

[10] This representation was independently proposed by GLASSER, A., LEE, Y.C., PEGORARO, F., SCHEP, T., in Proc. 1977 Varenna Workshop on Finite-β Plasmas (COPPI, B., SADOWSKY, W., Eds) Publisher: US Department of Energy, Washington, D.C., (1978).

[11] CONNOR, J.W., HASTIE, R.J., TAYLOR, J.B., Phys. Rev. Lett. **40** (1978) 396.

[12] WARE, A.A., HAAS, F.A., Phys. Fluids **9** (1966) 959.

[13] COPPI, B., FERREIRA, A., MARK, J.W.-K., SUGIYAMA, L., Massachusetts Institute of Technology (RLE) Report PRR 78/43, Cambridge, Mass. (December 1978).

[14] MERCIER, R., in Plasma Physics and Controlled Nuclear Fusion Research (Proc. 7th Int. Conf. Innsbruck, 1978) Vol. 1, IAEA, Vienna (1979) 701.

[15] SYKES, A., TURNER, M.F., FIELDING, P.J., HAAS, F.A., ibid., 625.

[16] ZAKHAROV, L.E., ibid., 689.

(Manuscript received 23 August 1978
Final version received 5 February 1979)